University of Nevada, Reno

Investigating Myosin Light Chain Kinase Binding with Actin in Human Airway Smooth Muscle Cells

A thesis submitted in partial fulfillment
of the requirements for the degree of

Bachelors of Science in Biochemistry and Molecular Biology Major

by

Avery Brown

Dr. Christine Cremo, Thesis Advisor

May, 2015

UNIVERSITY OF NEVADA RENO

THE HONORS PROGRAM

We recommend that the thesis
prepared under our supervision by

Avery Brown

entitled

Investigating Myosin Light Chain Kinase Binding with Actin in Human Airway Smooth Muscle Cells

be accepted in partial fulfillment of the
requirements for the degree of

BACHELOR OF SCIENCE, BIOCHEMISTRY AND MOLECULAR BIOLOGY

_____

Dr. Christine Cremo, Ph.D., Thesis Advisor

_____

Tamara Valentine, Ph.D., Director, Honors Program

May 2015

Abstract

Myosin light chain kinase plays an integral role in initiating and regulating smooth muscle contraction. These experiments were conducted to help illuminate and better understand the process by which myosin light chain kinase interacts with actin and myosin in the ventral stress fibers of permeabilized human airway smooth muscle cells. The first 75 residues of the N-terminal end of MLCK (GST tagged N75) contain the three DFRXXL motifs, which are sufficient for actin binding [1-4]. N75 binding to actin was imaged using fluorescence microscopy and total internal reflection microscopy under varying conditions. N75 binding was inhibited when cells were pre-treated with the S1 fragment of myosin heads. This suggests that the DFRXXL motifs of MLCK are competing with S1 for actin binding sites. These experiments help better the understanding of the role myosin light chain kinase plays in the regulation and contraction of smooth muscle contraction.

Table of Contents

List of Figures

Introduction

Smooth muscle contraction is regulated and initiated by myosin light chain kinase. Myosin light chain kinase is a ubiquitous calcium-calmodulin activated kinase found in smooth, cardiac and skeletal muscle as well as in mammalian non-muscle cells [1]. When myosin light chain kinase is activated, it can phosphorylate Serine 19 of the regulatory light chain of smooth muscle myosin [1]. The phosphorylation of smooth muscle myosin then activates the actin-activated myosin ATPase activity, which is necessary and sufficient for muscle contraction [1]. MLCK is in low abundance relative to the amount of myosin it phosphorylates. MLCK is also tightly bound to the contractile apparatus and the binding of Ca2+-CaM can be altered by a variety of factors. At the N-terminus of myosin light chain kinase is the actin binding site, which is composed of three DFRXXL motifs which bind weakly to actin [1-5]. The DFRXXL motifs are located at amino acid residues 2-7, 30-35, and 58-63 [4]. Deletion of any of the motifs decreases actin binding or eliminates it completely [1-7].

N75 is a GST tagged peptide that contains the first 75 amino acids of the N-terminus of full length MLCK. N75 demonstrates the same actin binding capabilities as full length MLCK [4-7]. By imaging and analyzing this peptide's interaction with actin filaments in human smooth muscle cells, the process by which full length MLCK interacts with the contractile apparatus and regulates smooth muscle contraction can be further understood. A better understanding of how MLCK operates would allow for a better molecular module of how smooth muscle contraction is initiated and regulated. Such knowledge could play a role in treating diseases such as high blood pressure and asthma [2].

Methods

Preparing Growth Media for Cells

Cellgro Media M199 was used. 500 ml of media were prepared with final concentrations of 10% newborn calf serum, .5ng/ml EGF, and 2ng/ml of FGF. All growth factors were purchased from Sigma Aldrich.

Preparing Differentiating Media

500 ml of Cellgro Media M199 were prepared with final concentrations of .1% newborn calf serum, .5 ng/ml EGF, 2 ng/ml FGF, and 1 ng/ml of TGF-Beta1.

Expressing N75 [3]

GST-N_{1-75}MLCK (the N-terminal actin-binding domain of MLCK, residues 1–75, with GST fused to the N-terminus) in pGEX-2TK was expressed in BL21 cells. Cultures (5 l) were grown in LB medium to an optical density of 0.4 prior to IPTG (0.1 mM) induction for 3 h. Bacterial pellets were suspended in 500 ml phosphate-buffered saline (PBS) containing leupeptin (2.5 ug/ml), pepstatin A (2.5 μ g/ml), and PMSF (0.1 mM). Lysozyme was added to 5 mg/l and the culture was stirred for 30 min at room temperature. DTT (5 mM) was added and the mixture was centrifuged at 30,000***g*** for 45 min; the supernatant was diluted 3-fold with PBS and 5 ml of a 1:1 slurry of glutathione-Sepharose 4FF beads in PBS was added. After gentle shaking for 30 min and centrifugation at 150***g*** for 5 min, the supernatant was removed and the beads were washed with 100 ml PBS. The binding to beads was repeated twice more. The three sets of beads were combined, poured into a column (1 cm $\times$ 20 cm), washed with 10 column

volumes of PBS, and eluted with 10 mM glutathione, 50 mM Tris‑HCl, pH 8, and 5 mM DTT. GST-N_{1-75}MLCK-containing fractions were identified by SDS-PAGE, pooled, and dialyzed against 30 mM Tris‑HCl, pH 7.5, 20 mM NaCl, 1 mM EGTA, and 0.1 mM DTT. Thrombin (Novagen, restriction grade) digestion (8 U/ μ l) was carried out for 2 h at room temperature and stopped by addition of 0.1 mM PMSF. The solution was clarified by centrifugation at 39,000***g*** for 30 min. The supernatant was applied to an SP-Sepharose column (1 cm $\times$ 10 cm), equilibrated with 30 mM Tris‑HCl, pH 7.5, 20 mM NaCl, 1 mM EGTA, and 0.1 mM DTT, at a flow rate of 25 ml/h. After unbound proteins were eluted, 0.5 M NaCl in the same buffer followed by a step to 1 M NaCl eluted the N_{1-75}MLCK. Fractions were identified by NEXT GEL™ (Amresco) electrophoresis (15% acrylamide); pooled and dialyzed against 30 mM Tris‑HCl, pH 7.5, 20 mM NaCl, 1 mM EGTA, and 0.1 mM DTT using 3.5 kDa cutoff dialysis tubing; concentrated in Aquacide II; and dialyzed again. Protein concentration was determined by the bicinchoninic acid assay. N_{1-75}MLCK has the following sequence (corresponding to the N-terminal domain of rabbit smooth muscle MLCK):**LVPR/GS**<u>RRASV</u>*GSGGG*MDFRANLQRQVKPKTVSEEERKVHSPQQVDFRSVL-AKKGTPKTPVPEKAPPPKPATPDFRSVLGSKKKLPAENGS. M_r = 9348 after thrombin cleavage. The / indicates a thrombin cleavage site, an engineered PKA phosphorylation site is underlined, and a linker to the beginning of the MLCK sequence is in italics.

Preparing Human Airway Smooth Muscle Cells for Imaging

Cells were plated on a .045 mg/ml collagen coated coverslip and allowed to differentiate for 3 days in differentiating growth media. Flow cells were created using the coverslip and microscope slides. Cells were then permeabilized with .1% triton and stained with .5 Mm trit-c.

Protocol for Imaging Cells and GST.

All washes were done with 85 microliters of fluid. N75 (1uM) and S1 were allowed to incubate for 15 minutes. Actin buffer contained 1/10th volume of actin polymerization buffer, 0.5 mM DTT. The concentration of the quantum dots was .25 nM and were incubated in the cells for 1 min. Observation buffer contained 100 ul of 10x buffer A, 500 ul of methyl cellulose, 380 ul water, 20 ul O2 scavengers. Imaging was done at 4 degrees Celsius. Observation buffer 2 contained 362 ul water, 18 ul of 111.7 mm ATP (2mM final concentration) 100 ul of 10x buffer A, 500 ul of methyl cellulose, and 20 ul O2 scavengers. Skeletal S1 was at a concentration of 37uM in buffer F. For figure 1, the protocol for imaging slides was as follows: N75 was added, then a wash with actin buffer, added Quantum Dots, then a wash with actin buffer, then adding observation buffer. For figure 2, the protocol for imaging slides was as follows: S1 added, then a wash with actin buffer, add N75, wash with actin buffer, add Quantum Dots, wash with actin buffer, then observation buffer. For figure 3, the protocol for imaging slides was as follows: NEM-S1 added, a wash with actin buffer, N75 added, wash with actin buffer, add Quantum Dots, wash with Actin Buffer, add observation buffer. For figure 4, the protocol for imaging slides was as follows: NEM-S1 added, wash with actin buffer, add

N75, wash with actin buffer, add Quantum Dots, wash with actin buffer, add observation buffer, flow in 3 ul of 111.7 mM ATP (During Imaging). For figure 5, the protocol for imaging slides was as follows: S1 added, wash with actin buffer, add N75, wash with actin buffer, add Quantum Dots, wash with actin buffer, add observation buffer (Contained 2mM ATP). For figure 6, the protocol for imaging slides was as follows: S1 added, wash with actin buffer, add N75, wash with actin buffer, add Quantum Dots, wash with actin buffer, add observation buffer (contained 2mM ATP), flow in N75 at time = 0 (during imaging).

Analyzing Cell Images and Movies

Movies were prepared using ImageJ.

Buffers. Actin buffer is 50 mM KCl, 50 mM imidazole (pH 7.4), 2 mM EGTA, 8 mM $MgCl_2$, 10 mM DTT, Actin imaging buffer is actin buffer with added oxygen scavengers (0.1 mg/ml glucose oxidase, 0.018 mg ml^{-1}catalase, 2.3 mg ml^{-1} glucose) and 0.5 % methylcellulose. Buffer *a* is 150 mM KCl, 4 mM $MgCl_2$, 2 mM EGTA, 10 mM DTT, 25 mM imidazole (pH 7.0). If used during imaging, the buffers also contained 0.5% methylcellulose and oxygen scavengers as above.

Microscopy. Images of fluorescent actin were recorded using a Nikon TE2000 epifluorescence microscope (Technical Instruments, CA) with a Roper Cascade 512B camera (Princeton Instruments, Trenton, NJ) with a 100X objective. Widefield excitation at 532 nm was with a Hg-Xe lamp and a Nikon 565 nm (TRITC) G-2E\C band –pass

emission filter. Image sequences (movies) of QD-labeled proteins were observed for 1-2 min by total internal reflection fluorescence (TIRF) using a 488 nm excitation wavelength. The frame rate for the TIRF movies was 5 s^{-1}. The merged images of the QD signal with TRITC signal from actin were generated using Image J (National Institute of Healthy, Bethesda, MD, USA). Movies or images were 512 x 512 pixels at a resolution of 106 nm pixel (54 x 54 µm).

Results

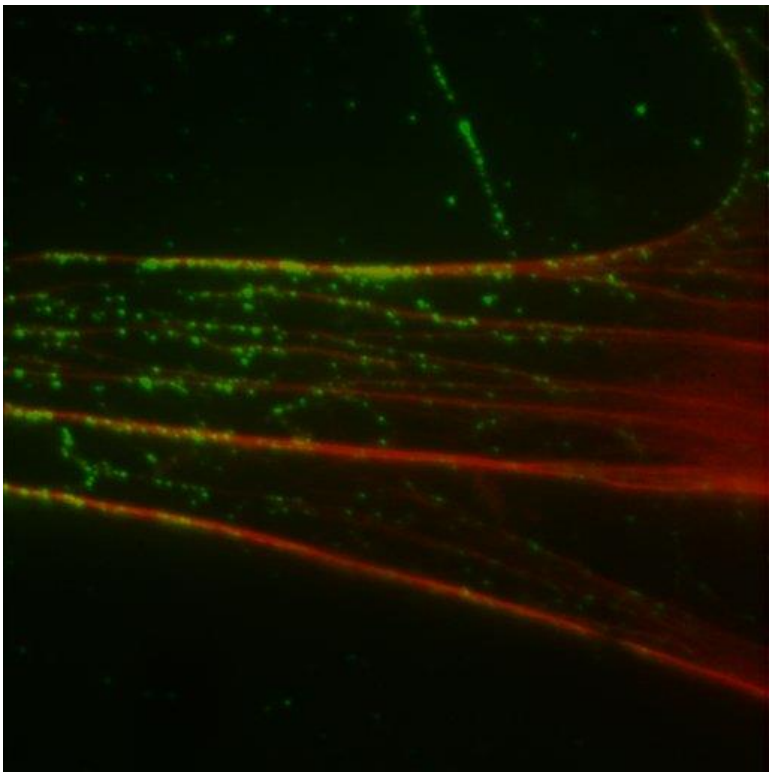

1A.

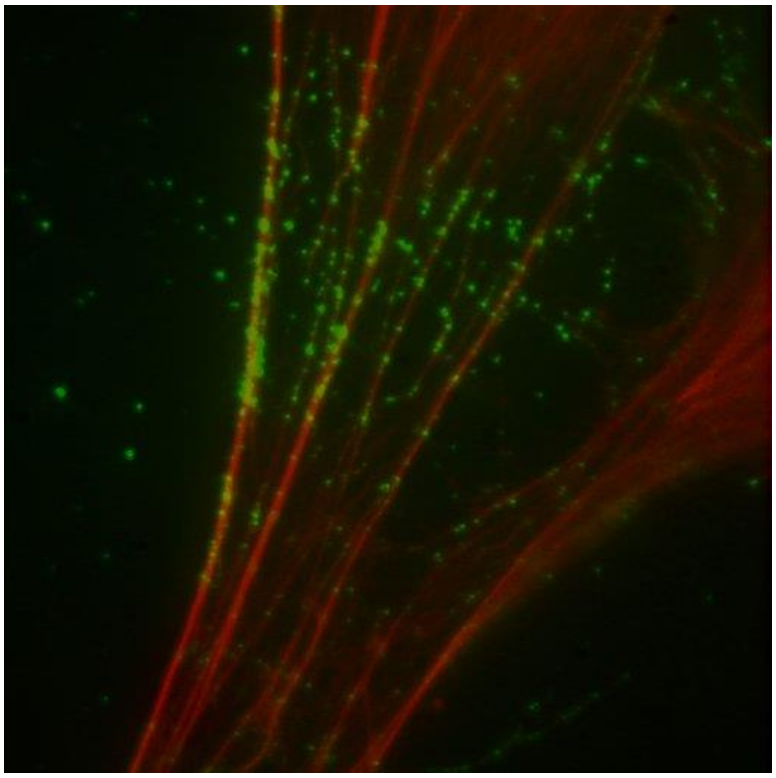

1B.

Figure 1. Colocalization of N75 to Stress Fibers in Human Airway Smooth Muscle Cells. N75 was allowed to bind for 15 minutes in permeablized cells before being washed out. The peptide was visualized through the use of quantum dots that contained strept avidin, which bound to biotin groups attached to the N75. The stress fibers are red and the quantum dots are green.

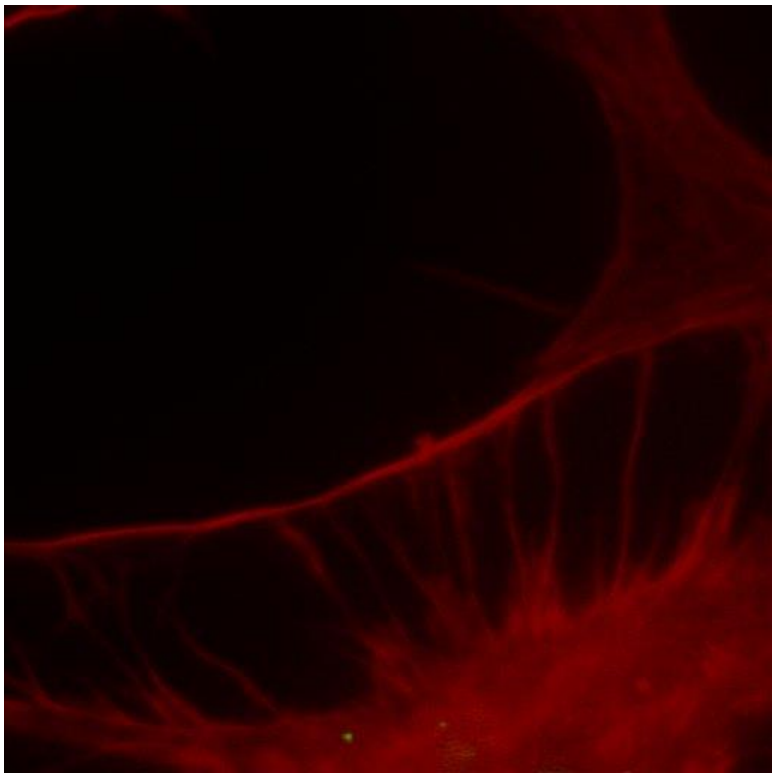

2A.

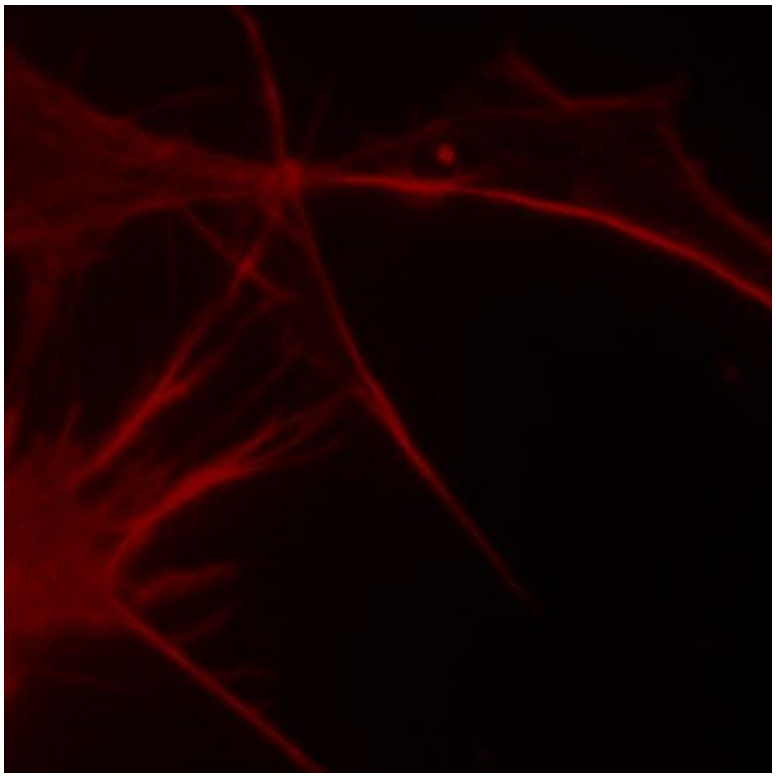

2B.

Figure 2. S1 Decreasing N75 Binding on Stress Fibers. Skeletal S1 was added to the cells before N75. There was a significant decrease in binding when stress fibers were pre treated with S1.

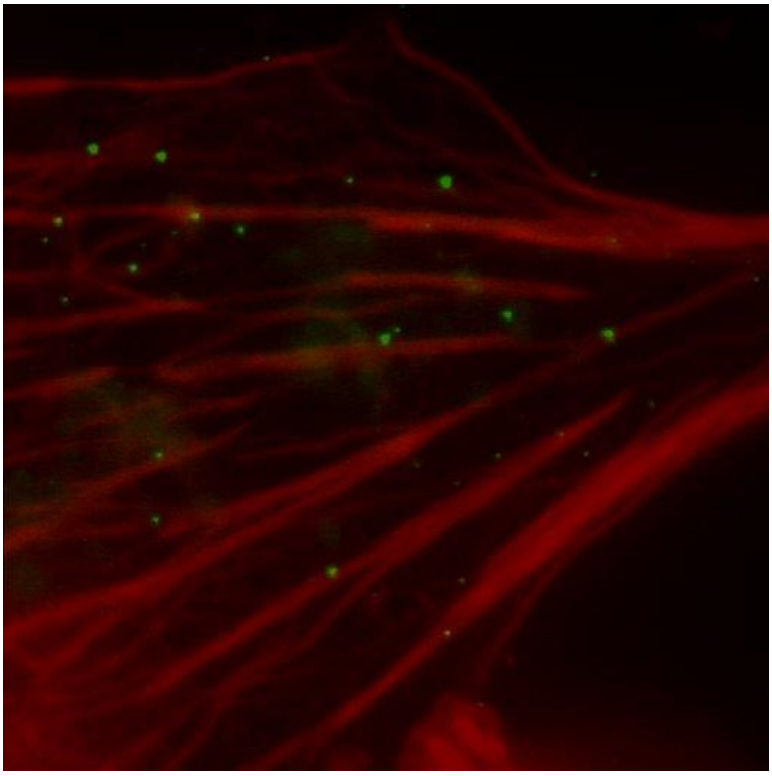

3A.

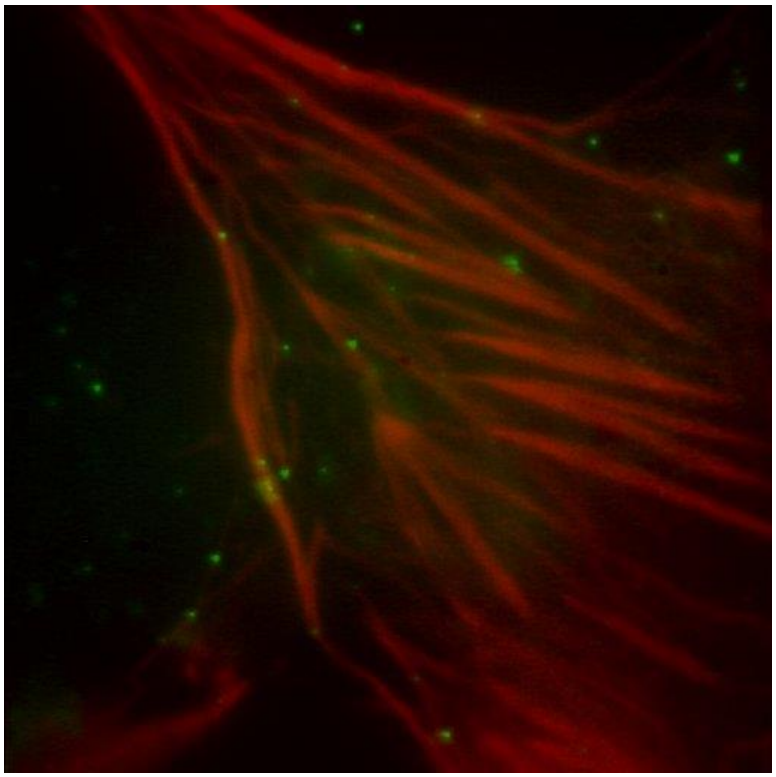

3B.

Figure 3. NEM-S1 Decreasing N75 Binding on Stress Fibers. NEM-S1 binds strongly to actin even in the presence of ATP. NEM-S1 was allowed to bind to the cells before N75. Similar to regular S1, there was a significant decrease in peptide binding on the stress fibers.

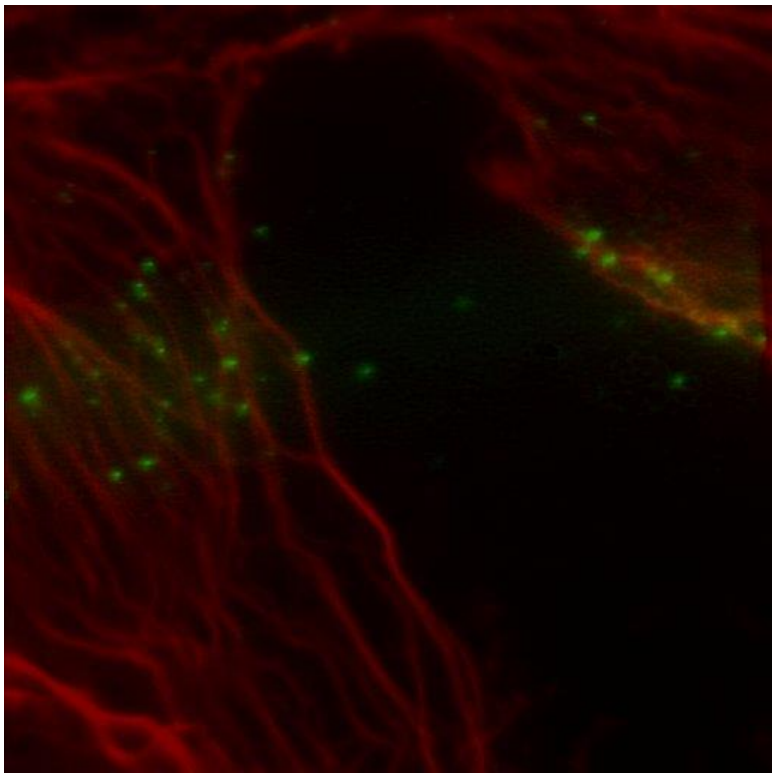

4A.

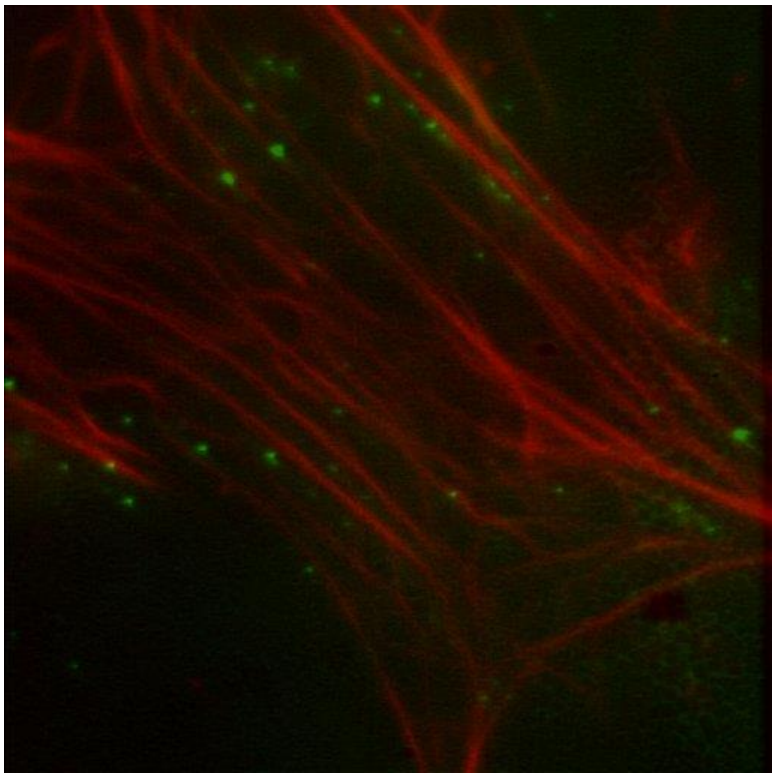

4B.

Figure 4. N75 Binding After NEM-S1 Allowed to Bind and ATP Added. NEM-S1 then N75 was allowed to bind to the stress fibers of the cell. During imaging, 3ul of 111.7 mM pure ATP was flowed into the cells to see if there would be an increase in N75 binding due to the dissociation of NEM-S1. There didn't seem to be a large increase in peptide binding.

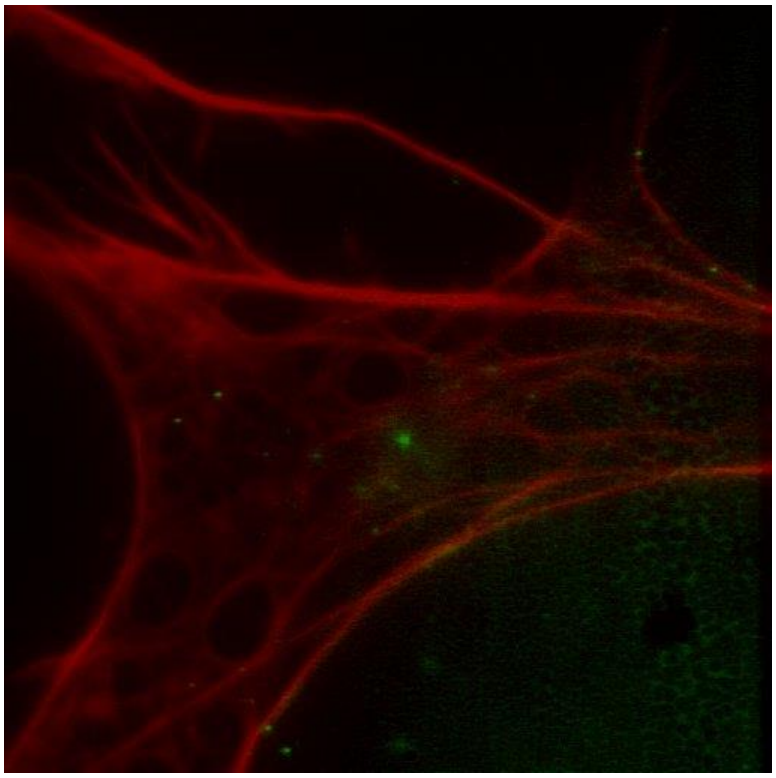

5A

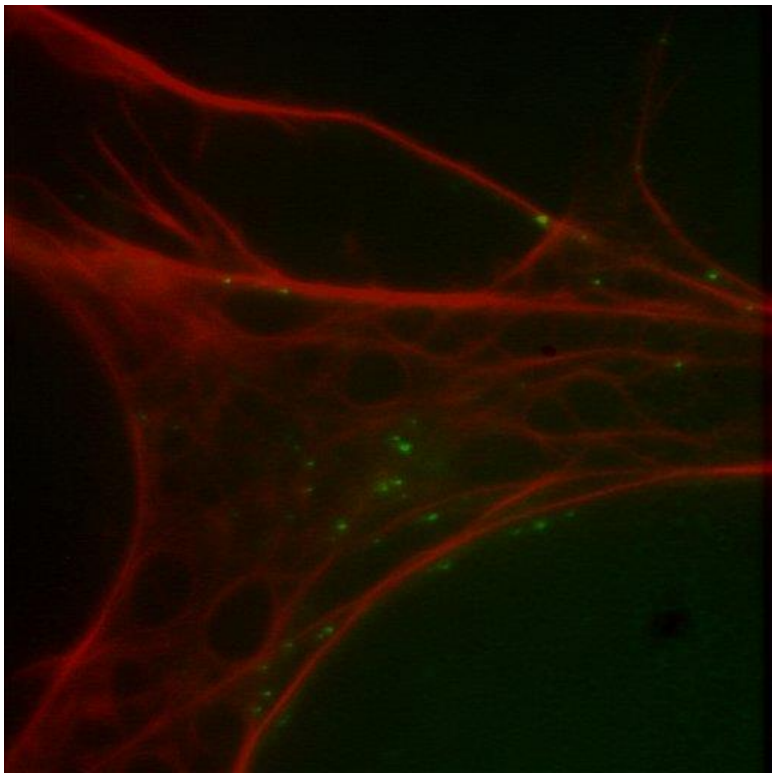

5B

Figure 5. Change in Binding When S1 Added to Cells With ATP in Imaging Buffer. S1 was added to the cells before N75. ATP (2mM) was in the observation buffer. The images show the change in binding of N75 after one hour. There seems to be a slight increase in binding after the addition of ATP.

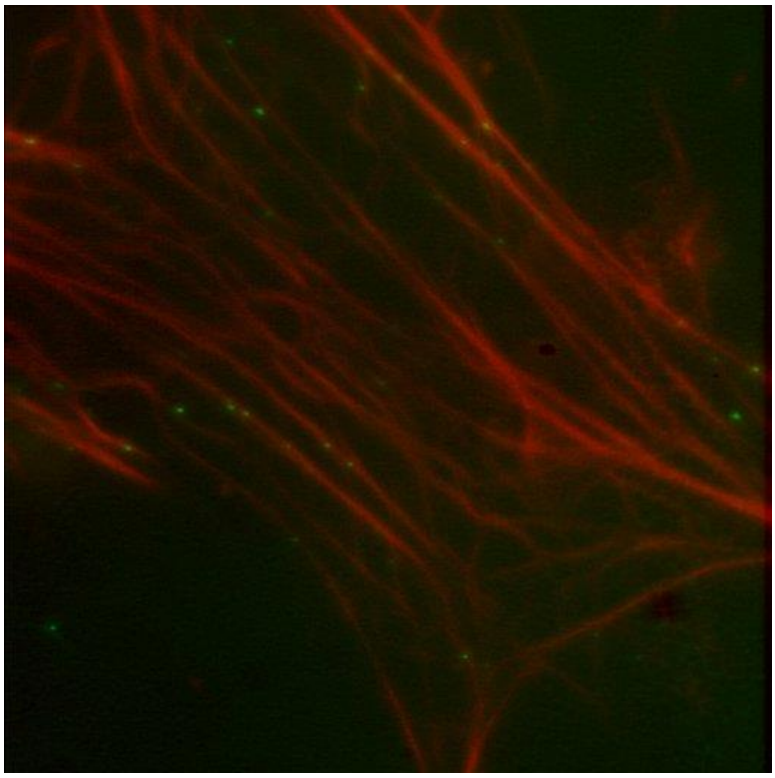

6A

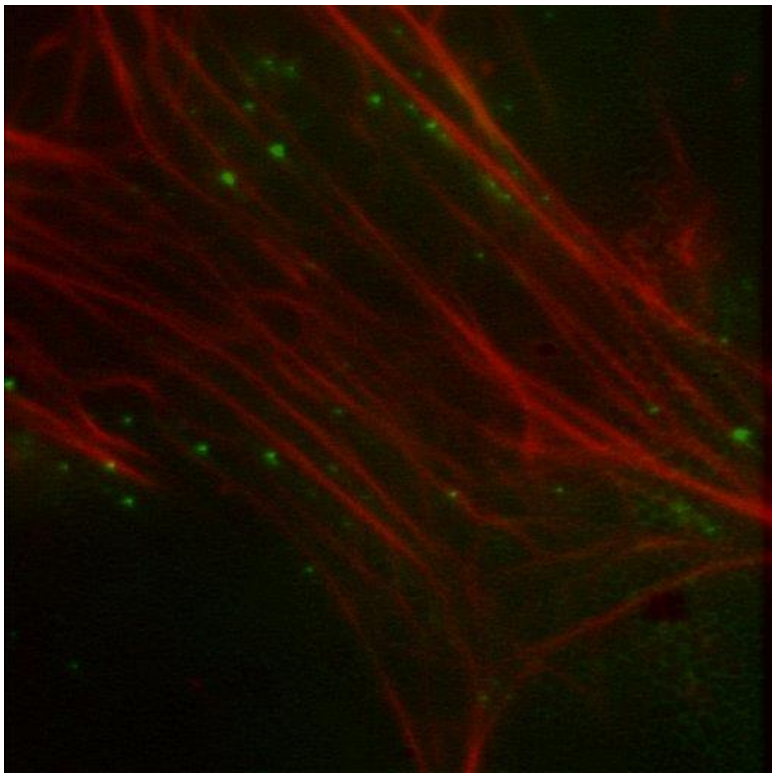

6B

Figure 6. Change in Binding When ATP Added After S1 and Additional N75 Flowed Into Cell. S1 was allowed to bind before N75. ATP (2mM) was in the observation buffer. During imaging, additional N75 (premixed with quantum dots) was flowed into the cell. Movies of the change in binding were taken for 10 minutes apart for 40 minutes. There seems to be a slight increase in peptide binding to the stress fibers.

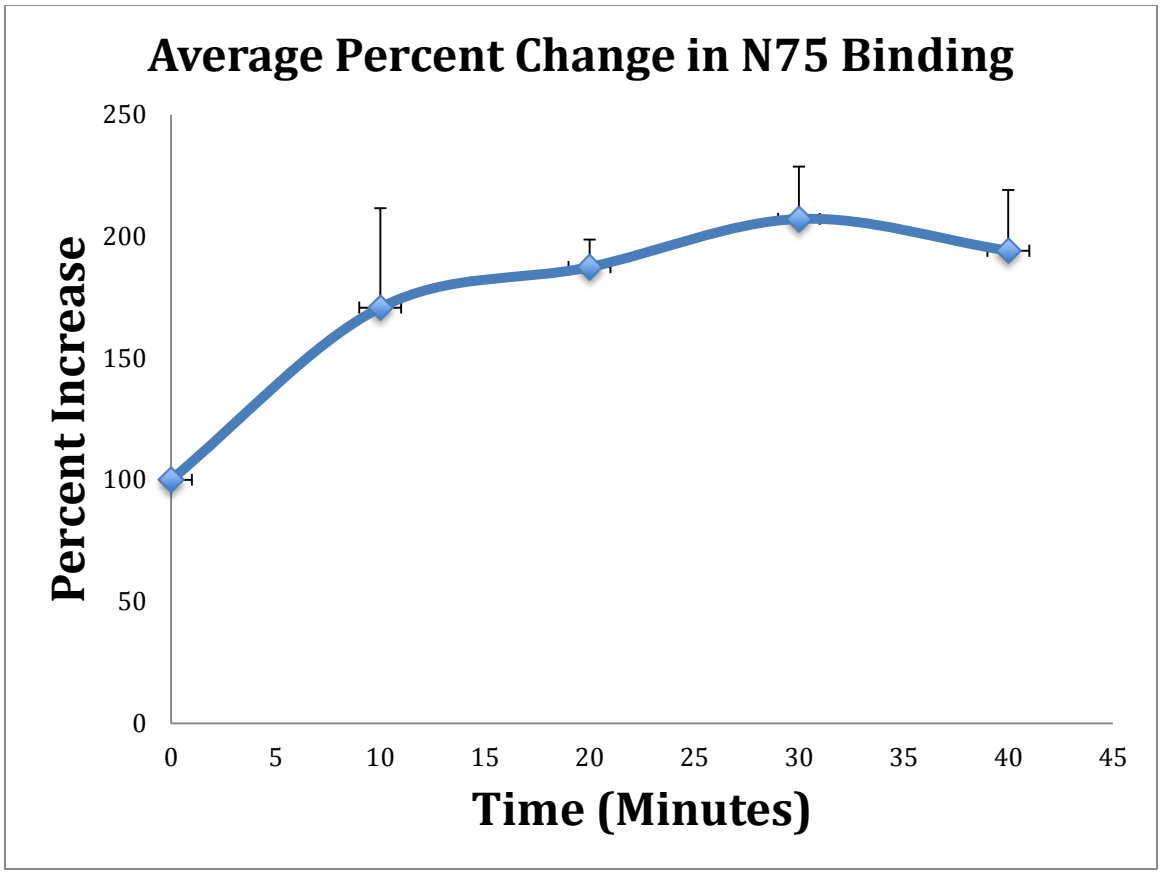

Figure 7. Change in N75 Binding in Cells with S1 and ATP Over 40 Minute Period. The experiment from figure 7 was repeated in six different cells on two separate days. At the start of the forty-minute period, additional N75 was flowed into the cells, which were pre-treated with S1 and had ATP added through the observation buffer. Binding events were measured by creating Z-stack images from the movies and counting the total number of quantum dots in each Z-stack. The average increase in binding and standard error was calculated for each ten-minute time point.

Results

Figure 1 shows cells that were treated with N75 for fifteen minutes and no S1. The peptide is clearly seen colocalizing to the stress fibers of the human airway smooth muscle cells. Figure 2 shows cells that were treated with S1 for fifteen minutes and then N75. There was a significant decrease in colocalization of the peptide to the stress fibers of the cells. This suggests that the binding site for myosin and S1 may be located closer to each other than previously believed. In order to test this, additional experiments were performed to tests whether S1 binding was influencing N75 binding. Figure 3 shows stress fibers that were treated with NEM-S1 for fifteen minutes before N75 was added. NEM-S1 binds strongly to actin and doesn't dissociate in the presence of ATP. The NEM-S1 showed similar results as the S1 treated cells. There was a significant decrease in N75 colocalization to the stress fibers of the cells. To test whether the NEM-S1 would continue to influence N75 binding even in the presence of ATP, 3 ul of 111.7 mM ATP was flowed into the cells during imaging. As expected, there didn't see to be a large change in binding. Figure 5 shows the change in binging over a one-hour period in cells that were treated with S1before N75 and had ATP added in the observation buffer 2(mM final concentration). There seems to be a slight increase in N75 binding, suggesting that the ATP is causing the S1 heads to dissociate from the stress fibers and allow N75 to interact. Figure 6 shows the change in binding of N75 when S1 was allowed to bind in the cells first and ATP (2mM final concentration) was in the observation buffer. During imaging, additional N75 was flowed into the cells. The slight increase in binding suggests that ATP was weakening the S1 interaction with actin in the stress fibers, which allowed the N75 to bind. Figure 7 shows the increase in binding over a one hour period. By the

end of the imaging period, there is almost twice as many binding events. These most likely occurred from some quantum dots showing up better in later movies but were undistinguishable in earlier movies.

Discussion

Previous studies have shown that all three DFRXXL regions are important for actin binding [4]. An unresolved issue has been whether the motifs bind directly to F-actin in smooth muscle myofilaments or in actin containing stress fibers in cells. The significant decrease in binding seen in Figure 2 suggests that these regions do directly bind to actin containing stress fibers because S1 has effectively stopped the peptide and actin from interacting. Previous studies also suggest that the three DFRXXL motifs each bind one actin monomer in actin filaments [5, 7]. Previous studies also suggests that the binding site of MLCK is distinct from any other actin binding protein and that this unique binding site hasn't had another actin binding protein localized to the site [4, 5, 7]. The results of this study show that N75 and S1 compete for binding sites. This is suggested by the decrease in N75 binding after S1 was allowed to bind. It's also suggested by the slight increase in peptide binding when ATP is introduced to the cells and causes S1 to dissociate. The difference between the referenced studies and these experiments was the use of stress fibers in human airway smooth muscle cells instead of purified F-actin. Future experiments to further investigate the binding sites of S1 and N75 would be to repeat the experiments on purified F-actin or add N75 to the stress fibers and then fluorescent labeled myosin S1 heads.

References

1. Hong, F., et al. "Biochemistry of Smooth Muscle Myosin Light Chain Kinase." *Arch Biochem Biophys* 510.2 (2011): 135-46. Print.

2. Ye, L. H., et al. "The Structure and Function of the Actin-Binding Domain of Myosin Light Chain Kinase of Smooth Muscle." J Biol Chem 272.51 (1997): 32182-9. Print.

3. Stull, J. T., et al. "Myosin Light Chain Kinase: Functional Domains and Structural Motifs." *Acta Physiol Scand* 164.4 (1998): 471-82. Print.

4. Smith, Lula et. al. "Identification of a Novel Actin Binding Motif in Smooth Muscle Myosin Light Chain Kinase." *J Biol Chem* 274.41 (1999): 29433-8. Print.

5. Hatch, V., et al. "Myosin Light Chain Kinase Binding to a Unique Site on F-Actin Revealed by Three-Dimensional Image Reconstruction." *J Cell Biol* 154.3 (2001): 611-7. Print.

6. Kanoh, Satoshi, et al. "Actin-Binding Peptide from Smooth Muscle Myosin Light Chain Kinase." *Biochemistry* 32 (1993): 8902-07. Print.

7. Smith, L., et al. "Properties of Long Myosin Light Chain Kinase Binding to F-Actin in Vitro and in Vivo." *J Biol Chem* 277.38 (2002): 35597-604. Print.

8. Haldeman, B. D., et al. "The Kinetics Underlying the Velocity of Smooth Muscle Myosin Filament Sliding on Actin Filaments in Vitro." *J Biol Chem* 289.30 (2014): 21055-70. Print.

9. Hong, F., et al. "Kinetics of Myosin Light Chain Kinase Activation of Smooth Muscle Myosin in an in Vitro Model System." *Biochemistry* 52.47 (2013): 8489-500. Print.

10. Hong, F., BD Haldeman, OA John, PD Brewer, YY Wu, S. Ni, DP Wilson, MP Walsh, JE Baker, and CR Cremo. "Characterization of Tightly Associated Smooth Muscle Myosin-Myosin Light-Chain Kinase-Calmodulin Complexes." *J Mol Biol* 390.5 (2009): 879-92. Print.

11. Kohama, Kazuhiro Sasaki Yasuharu. *Molecular Mechanisms of Smooth Muscle Contraction*. 1999. *Molecular biology intelligence unit; Variation: Molecular biology intelligence unit.*Web <http://public.eblib.com/EBLPublic/PublicView.do?ptiID=226284><Materials specified: Ebook Library http://public.eblib.com/EBLPublic/PublicView.do?ptiID=226284>.

12. Mabuchi, Y., et al. "Modular Structure of Smooth Muscle Myosin Light Chain Kinase: Hydrodynamic Modeling and Functional Implications." *Biochemistry* 49.13 (2010): 2903-17. Print.

13. Noonepalle, Satishkumar. "Construction of Recombinant Rabbit Uterine Smooth Muscle Myosin Light Chain Kinase Cdna for Expression in Insect Cells." Print.

14. Tan, John L. "Regulation of Myosin Ii by Light Chain Phosphorylation: Studies on the Dictyostelium Myosin Light Chain Kinase." Print.

15. Trybus, K. M., and S. Lowey. "Conformational States of Smooth Muscle Myosin. Effects of Light Chain Phosphorylation and Ionic Strength." *J Biol Chem* 259.13 (1984): 8564-71. Print.

16. Walsh, M. P. "Vascular Smooth Muscle Myosin Light Chain Diphosphorylation: Mechanism, Function, and Pathological Implications." *IUBMB Life* 63.11 (2011): 987-1000. Print.